

## Metal Atom Incorporation Studies on the Phases with NZP Structure: $\square\text{NbTiP}_3\text{O}_{12}$ \*

G. V. SUBBA RAO, U. V. VARADARAJU, AND K. A. THOMAS

*Materials Science Research Centre, Indian Institute of Technology, Madras 600 036, India*

AND B. SIVASANKAR

*Department of Chemical Engineering, A. C. College of Technology, Anna University, Madras 600 025, India*

Received December 29, 1986; in revised form March 23, 1987

A wide variety of electropositive elements of the periodic table can be inserted into the vacant sites in the host framework structure of hexagonal  $\text{NbTiP}_3\text{O}_{12}$  (an analog of nasicon) to give rise to isostructural phases. Synthesis, characterization, and preliminary data on the structure, IR spectra, and electrical resistivity are presented. Possible areas for further exploration are delineated. © 1987 Academic Press, Inc.

### Introduction

Solid compounds possessing 2-D layer (with a van der Waals gap) and 3-D framework (with interconnected channels) structures provide the interesting possibility of the incorporation (intercalation) of foreign metal atoms into the host lattice giving rise to new isostructural compounds with novel physical properties. This, however, usually occurs when the metal atom in the host lattice can exhibit a variable valency. Examples are layered transition metal dichalcogenides (1-3), ternary molybdenum chalcogenides (Chevrel phases) (3-5), binary transition metal oxides (6, 7), and ternary oxides with spinel (8) or defect pyrochlore structure (9) and similar other 3-D-network structures (10).

Nasicon,  $\text{Na}_3\text{Zr}_2\text{Si}_2\text{PO}_{12}$ , represents an example of a mixed oxide with a 3-D framework with interconnected channels and has evoked considerable interest in recent years due to its Na fast ion conduction properties (11, 12). It belongs to the class of NZP ( $\text{NaZr}_2\text{P}_3\text{O}_{12}$ ) phases with the general formula  $A^{1+}M_2^{4+}\text{P}_3\text{O}_{12}$  possessing a hexagonal symmetry. The structure consists of a 3-D network of  $\text{PO}_4$  tetrahedra sharing corners with  $\text{ZrO}_6$  octahedra and a 3-D-linked interstitial space occupied by A ions. There are two different sites for the A ions: Type I sites (6b) situated between two  $\text{ZrO}_6$  octahedra along the c-axis ("ribbons" of  $\text{O}_3\text{ZrO}_3\text{NaO}_3\text{ZrO}_3$ ) with a distorted octahedral coordination and Type II sites (18e) located between the ribbons (perpendicular to c-axis) with a trigonal prismatic coordination. The ribbons are connected by  $\text{PO}_4$  tetrahedra along the a-axis (13). In NZP,

\* Dedicated to Franz Jellinek.

the Type I sites are completely filled whereas, in nasicon, Type I sites are filled and Type II sites are partially filled. The NZP structure is versatile in that chemical substitution is possible at Na, Zr, and P sites by a variety of elements to give rise to a large number of isostructural phases, including vacancy at A site (e.g.,  $\square MM'P_3O_{12}$ ;  $M = \text{Nb, Ta, Sb}$ ;  $M' = \text{Ti, Zr, Hf, Ge}$ ) (11–14). Thus, the NZP framework provides an ample scope for tailoring the physical properties which include (i) fast ion conduction when  $A = \text{Li or Na}$  and (ii) controlled or zero thermal expansion coefficient (TEC) ceramics (15).

Recently, we have shown (16) that Li can be incorporated into the NZP phases provided there are chemically reducible species in the host lattice, e.g., Ti, Nb. Thus Li has been inserted, using *n*-butyllithium, at room temperature into  $\text{LiTi}_2\text{P}_3\text{O}_{12}$  and  $\square\text{NbTiP}_3\text{O}_{12}$  ( $\square$ , vacancy) resulting in singly and doubly lithiated compounds with resultant changes in the structure and IR spectral properties. However, the changes are not very pronounced in the lithiated  $\text{NbTiP}_3\text{O}_{12}$ , possibly due to the filling-up of Type I sites and small ionic size of lithium. Presently we have succeeded in incorporating other electropositive metals into  $\text{NbTiP}_3\text{O}_{12}$ . Preliminary results on their synthesis, characterization, resistivity and IR data are presented.

## Experimental

The parent compound  $\square\text{NbTiP}_3\text{O}_{12}$  was prepared by the high-temperature solid state reaction in air (1200°C) starting from high purity  $\text{Nb}_2\text{O}_5$  (99.9%; NFC, Hyderabad, India),  $\text{TiO}_2$  (99.5%; Riedel, West Germany), and  $\text{NH}_4\text{H}_2\text{PO}_4$  (>99%; recryst., Sarabhai, India). The stoichiometric mixtures of the above were mixed thoroughly and heated at 200°C for 10–12 hr to decompose the  $\text{NH}_4\text{H}_2\text{PO}_4$ , 600°C for 4–6 hr and 900°C for 12–15 hr. The mixtures

were then pelletized (4 tonnes/cm<sup>2</sup>) and heated at 1000°C for 4–5 hr and finally at 1300°C for 12 hr. The phases were characterized by powder X-ray diffraction (XRD). The LSQ-fitted hexagonal lattice parameters are in good agreement with the values reported in literature (13). Metal atom insertion was affected by solid state reaction of  $\text{NbTiP}_3\text{O}_{12}$  with the respective metals in their elemental form at elevated temperatures (800–900°C) in evacuated ( $10^{-5}$  Torr) and sealed quartz tubes (10 mm diam, Thermal Syn., UK). Stoichiometric quantities of the metal powder or turnings (purity >99.99%; Ventron, USA, or Cerac, UK or SMP, NFC, Hyd., India) and the  $\text{NbTiP}_3\text{O}_{12}$  were mixed thoroughly and pelletized prior to heat treatment. Repeated grinding and heating was necessary to obtain single phase materials. Powder XRD data were obtained using a Philips unit ( $\text{CuK}\alpha$ ; Ni-filter). Hexagonal lattice parameters were obtained by the LSQ fitting of the powder data using computer programs. The LAZY PULVERIX computer program was used (IBM-370) to compute the calculated X-ray intensities from the known atom positions. Electrical conductivity was measured on polycrystalline sintered disks using a two-probe apparatus. IR spectra were recorded in the range 4000–200  $\text{cm}^{-1}$  as KBr or polyethylene disks (Perkin-Elmer 983). Thermal gravimetric analysis (TGA) studies were done in  $\text{N}_2$  or air using Mettler (TA-3000) unit.

## Results and Discussion

### A. Stability and Structure

A partial periodic table of the electropositive elements that have been incorporated into  $\text{NbTiP}_3\text{O}_{12}$  is shown in Fig. 1. The value of  $x$  in  $A_x\text{NbTiP}_3\text{O}_{12}$  is varied from 0.20 to 1.0 depending on the A metal. The colors of the compounds vary from gray to blue-black or black depending on the A

|    |    |    |    |    |    |    |    |    |    |    |    |    |    |    |    |    |
|----|----|----|----|----|----|----|----|----|----|----|----|----|----|----|----|----|
| Li | Be |    |    |    |    |    |    |    |    |    |    |    |    |    | Al | Si |
| Na | Mg |    |    |    |    |    |    |    |    |    |    |    |    |    |    |    |
| K  | Ca | Sc | Ti | V  | Cr | Mn | Fe | Co | Ni | Cu | Zn | Ga | Ge |    |    |    |
| Rb | Sr | Y  | Zr | Nb | Mo | Tc | Ru | Rh | Pd | Ag | Cd | In | Sn |    |    |    |
| Cs | Ba | La | Hf | Ta | W  | Re | Os | Ir | Pt | Au | Hg | Tl | Pb |    |    |    |
|    |    |    |    |    |    |    |    |    |    |    |    |    |    | Gd |    |    |

FIG. 1. Partial periodic table of the elements incorporated into □NbTiP<sub>3</sub>O<sub>12</sub>. Single-phase materials were obtained except when A = Ni, Cu, Ag, and Hg under the preparative conditions employed (800–900°C) (see text).

metal and its stoichiometry ( $x$ ), while pure NbTiP<sub>3</sub>O<sub>12</sub> is white in color. The color is due to the reduction of Nb<sup>5+</sup> and/or Ti<sup>4+</sup> to a lower oxidation state as noted in our earlier studies on lithiation into LiTi<sub>2</sub>P<sub>3</sub>O<sub>12</sub> and NbTiP<sub>3</sub>O<sub>12</sub> (16). Indeed, the color of the phase is black for higher values of  $x$  for a given A. The phases are stable toward exposure to air and moisture at room temperature. Long-term exposure, however, produces surface oxidation and hence the compounds are stored in a desiccator. They are also stable toward heating in an inert (N<sub>2</sub> or Ar) atmosphere. However, heating in air or O<sub>2</sub> to >400°C decomposes the compounds with the resultant decoloration. Formation of the metal oxide (AO, A<sub>2</sub>O<sub>3</sub>, etc.) has been established by the TGA technique.

Optimal temperatures for the preparation of various metal inserted NbTiP<sub>3</sub>O<sub>12</sub> phases have not yet been established. We may point out that this is necessary, especially in the case of metals having low melting points (e.g., Zn, Cd, In) where higher temperatures of heat treatment can lead to the metal oxide or metal phosphate formation with partial destruction of the crystal lattice. Similarly, the stoichiometries of the inserted metal atoms are chosen ("optimum") to give rise to A<sup>n+</sup> ion in the maximum possible oxidation state (e.g., Mg<sup>2+</sup>, In<sup>3+</sup>) and effect a one- or two-electron re-

duction of Nb<sup>5+</sup> and/or Ti<sup>4+</sup> in the host lattice ( $x = 0.5, 1.0$  and  $0.33$  and  $0.67$  respectively). However, when A is a transition metal ( $3d$  or  $4d$ ), it is necessary to establish the oxidation state by complimentary  $\chi$ -T, EPR and related studies. In the case of A = Mg, Zn, and Y, we tried to prepare the insertion compounds with  $x = 1.5, 1.5,$  and  $1.0,$  respectively. Under the conditions of preparation (800°C), impurity phases corresponding to Mg<sub>2</sub>P<sub>2</sub>O<sub>7</sub>, Y<sub>2</sub>O<sub>3</sub>, and YPO<sub>4</sub> were noted, in addition to the desired phase. This indicates that further reduction of Nb<sup>4+</sup> or Ti<sup>3+</sup> does not occur and that the excess metal partially disintegrates the crystal lattice. This observation is in agreement with our earlier results on lithiation of LiTi<sub>2</sub>P<sub>3</sub>O<sub>12</sub> and NbTiP<sub>3</sub>O<sub>12</sub> in that a maximum of two Li atoms was found to enter the lattice (16). We must point out that minor impurity phases were also noticed in some cases. This can be rationalized on the assumption that in a complex solid-solid reaction, there will always be competition between the diffusion of the A metal into the vacant lattice sites and the chemical reaction with the nonmetallic components of the host lattice. Unless the preparation temperatures are optimized, undesirable reaction products (impurity phases) are always formed. This has been amply demonstrated in the "metal-insertion" reactions in layered dichalcogenides (2, 3) and in Chevrel phases (3–5, 17).

The LSQ-fitted hexagonal lattice parameters of pure and metal-inserted NbTiP<sub>3</sub>O<sub>12</sub> are presented in Table I. The XRD patterns of NbTiP<sub>3</sub>O<sub>12</sub> and Fe compound are shown in Fig. 2. The parent phase  $hkl$  reflections are more or less retained in all the metal-inserted phases, indicating that the hexagonal symmetry is being retained. It is known that a monoclinic distortion is induced only when the Type II sites are partially or completely filled (e.g., nasicon and Li<sub>3</sub>Ti<sub>2</sub>P<sub>3</sub>O<sub>12</sub>) (11, 12, 16, 18). In NZP and related phases

TABLE I  
CRYSTAL, RESISTIVITY, AND IR DATA ON PURE AND METAL-INSERTED  $\text{NbTiP}_3\text{O}_{12}$

| Compound $A_x\text{NbTiP}_3\text{O}_{12}$ |                  | Hexagonal lattice parameter ( $\pm 0.05 \text{ \AA}$ ) |                    | Resistivity, $\rho$ ( $\Omega \text{ cm}$ ) | IR band positions and assignments ( $\pm 5 \text{ cm}^{-1}$ ) <sup>a</sup> |                                       |   |                     |                     |                |
|---|------------------|--|--------------------|---|--|---------------------------------------|---|---------------------|---------------------|----------------|
| A   | x                | a ( $\text{\AA}$ )                                     | c ( $\text{\AA}$ ) |   | $\nu_3(\nu_{\text{assym}}(\text{P-O}))$                                    | $\nu_1(\nu_{\text{sym}}(\text{P-O}))$ | $\nu_4(\nu_{\text{assym}}(\text{P-O}))$ | $\nu(M-O), A-O$     |                     |                |
| —   | —                | 8.56   | 21.92              | $1.8 \times 10^9$                           | 1265m<br>1071vs  | 1220m<br>998s                         | 922s                                    | 632vs,sp            | 581m                | 375vs          |
| Li  | 1.0 <sup>b</sup> | 8.50   | 22.39              | —   | —  | —                                     | —                                       | —                   | —                   | —              |
| Li  | 2.0 <sup>b</sup> | 8.53   | 22.43              | —   | 1265m<br>1075vs  | 1220m<br>998s                         | 925s                                    | 635vs,sp            | 576m                | 380vs          |
| Mg  | 0.5              | 8.60   | 21.71              | —   | 1220m  | 1058vs                                | 918m                                    | 635s,sp             | 602m,sp             | 370vs          |
| Mg  | 1.0              | 8.63   | 21.51              | $4.8 \times 10^7$                           | 1180m  | 1035vs                                | 915m                                    | 634s,sp             | 600s,sp             | 370vs          |
| Sn  | 0.5              | 8.56   | 22.84              | —   | 1215m  | 1018vs                                | 902vs                                   | 632vs,sp            | 550m,sp             | 383vs, 363vs   |
| Pb  | 0.5              | 8.57   | 22.76              | $5.1 \times 10^8$                           | 1220m<br>1020vs  | 1070vs                                | 900vs                                   | 633vs,sp            | 555m                | 383vs, 359vs   |
| Zn  | 0.5              | 8.53   | 21.53              | $3.1 \times 10^6$                           | 1215m  | 1050s                                 | 920s                                    | 632s,sp<br>570m     | 602s,sp             | 365vs          |
| Mn  | 0.5              | 8.64   | 21.32              | $1.7 \times 10^7$                           | 1228m<br>1059vs  | 1125vs<br>1000vs                      | 928vs                                   | 640s,sp             | —                   | 392vs, 368vs   |
| Y   | 0.33             | 8.62   | 22.01              | $1.5 \times 10^7$                           | 1220s<br>992vs   | 1070vs                                | —                                       | 665vs,sp<br>562s,sp | 632vs,sp<br>528m,sp | —              |
| Y   | 0.66             | 8.58   | 21.96              | —   | 1172s<br>990vs   | 1075vs                                | —                                       | 665vs,sp<br>560s,sp | 635vs,sp<br>528m,sp | —              |
| Gd  | 0.33             | 8.59   | 21.97              | —   | 1265m<br>1165s<br>1072vs   | 1225s<br>1110s<br>995s                | 920m                                    | 667m,sp<br>578m     | 632s,sp             | 370vs          |
| Fe  | 0.33             | 8.63   | 21.40              | —   | 1225m<br>998vs   | 1059vs                                | 925vs                                   | 638vs,sp            | —                   | 375vs          |
| Fe  | 0.66             | 8.63   | 21.20              | $1.9 \times 10^6$                           | 1220m  | 1032vs                                | 909m                                    | 638vs,sp<br>565m,sp | 593s,sp             | 375vs, 283s,sp |
| Ti  | 0.25             | 8.53   | 21.82              | $3.9 \times 10^5$                           | 1265m<br>1112s<br>992s   | 1220s<br>1072vs                       | 920s                                    | 632s,sp<br>515m     | 578m                | 370vs          |
| Ti  | 0.50             | 8.58   | 22.11              | $1.9 \times 10^4$                           | 1265m<br>1170s<br>990s   | 1220s<br>1070vs                       | 920s                                    | 665m,sp<br>560m,sp  | 632s,sp<br>525m     | 365vs          |
| Nb  | 0.20             | 8.60   | 22.17              | —   | 1269m<br>1115s<br>991s   | 1220s<br>1072vs                       | 915s                                    | 665m,sp<br>575m     | 632s,sp             | 369vs          |

<sup>a</sup> Only prominent bands listed. m, med; s, strong; vs, very strong; sp, sharp.

<sup>b</sup> From Ref. (16).

where the Type I site is either partially or completely filled, the undistorted hexagonal symmetry is retained. In the series of compounds presently synthesized,  $x$  in  $A_x\text{NbTiP}_3\text{O}_{12}$  is always  $< 1.0$ . Metal insertion produces changes in hexagonal lattice parameters (Table I) and changes in the relative intensities of select  $hkl$  peaks in the XRD patterns and lifting of the degeneracy or merger of the otherwise split lines (e.g., (104, 110), (116, 211), and (030, 214) peaks in Fig. 2). The XRD patterns when  $A_{0.5} =$

Sn and Pb are almost identical but qualitatively different from those when  $A = \text{Mg}$ , Zn, Mn, or Y with respect to the intensity distribution of  $hkl$  lines. However, they do resemble the original host lattice pattern and we have indexed the patterns on a hexagonal basis. More detailed XRD studies are necessary with regard to post-transition metal (e.g., Sn, Pb, In, Cd) insertion compounds.

From Table I we note that metal insertion does not produce much change in the  $a$  lat-

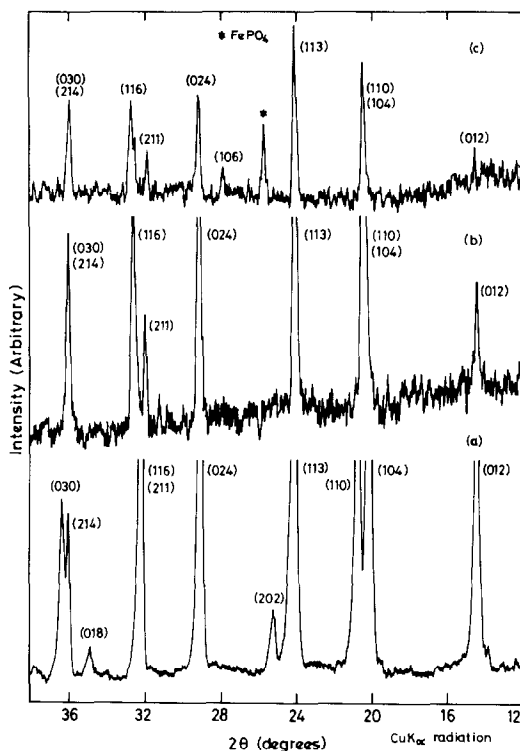


FIG. 2. XRD patterns of pure and Fe inserted  $\text{NbTiP}_3\text{O}_{12}$ . (a)  $\text{NbTiP}_3\text{O}_{12}$ , (b)  $\text{Fe}_{0.33}\text{NbTiP}_3\text{O}_{12}$ , and (c)  $\text{Fe}_{0.67}\text{NbTiP}_3\text{O}_{12}$ .

tice parameter while the  $c$  parameter is affected. This is as expected if the  $A$  metal occupies the Type I site and not the Type II site. When  $A = \text{Mg}, \text{Zn}, \text{Mn},$  and  $\text{Fe}$ , the  $c$  parameter decreases in comparison to pure  $\text{NbTiP}_3\text{O}_{12}$  and also with increasing  $x$ . For  $A = \text{Y}$  and  $\text{Gd}$ , either there is no change or there is a slight increase in the  $c$ -axis. Changes in  $a$  and  $c$  are related to the valency of the metal, its ionic size, and its electropositive character. At this stage, the available data are insufficient to draw conclusions regarding the systematic change in  $a$  and  $c$  with the inserted  $A$  metal and its stoichiometry.

### B. Infrared Spectra

IR spectra of many of the NZP analogs have been well documented and assign-

ments of  $\text{PO}_4$ ,  $\text{MO}_6$ , and  $\text{AO}_6$  bond-stretching and -bending vibrations have been done (19). However,  $\text{NbTiP}_3\text{O}_{12}$  and related vacancy containing phases have not been studied. Here we have examined the IR spectra of pure and metal-inserted phases in the range  $1400\text{--}200\text{ cm}^{-1}$ . The spectra are shown in Fig. 3 and important band positions and assignments (19) are listed in Table I. Distinct changes are noticed in the spectrum of  $\text{NbTiP}_3\text{O}_{12}$  after metal insertion, depending on the nature of the metal and stoichiometry, in the regions corresponding to the  $\text{PO}_4$  tetrahedral-stretching and -bending frequencies ( $1050\text{--}900, 650\text{--}550, 400\text{ cm}^{-1}$ ). Relatively minor changes occur in the region  $370\text{--}350\text{ cm}^{-1}$ , corresponding to the  $\text{MO}_6$  and  $\text{AO}_6$  octahedra. While distinct changes are noted in the re-

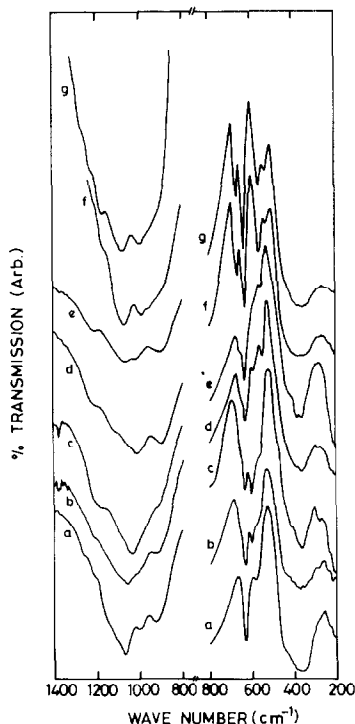


FIG. 3. IR spectra of  $A_x\text{NbTiP}_3\text{O}_{12}$ .  $A_x$ : (a)  $\square$ , (b)  $\text{Mg}_{0.5}$ , (c)  $\text{Mg}_{1.0}$ , (d)  $\text{Sn}_{0.5}$ , (e)  $\text{Pb}_{0.5}$ , (f)  $\text{Y}_{0.33}$ , and (g)  $\text{Y}_{0.67}$ .

gion 650–550  $\text{cm}^{-1}$  when  $A = \text{Mg}_{0.5}$  and  $\text{Mg}_{1.0}$ , the spectra remain the same for  $A = \text{Y}_{0.33}$  and  $\text{Y}_{0.67}$ . Similarly, the spectra are almost identical when  $A = \text{Sn}$  and  $\text{Pb}$  ( $x = 0.5$ ) but distinctly different from other  $A$  elements including pure  $\text{NbTiP}_3\text{O}_{12}$ . Detailed analysis is underway.

### C. Electrical Properties

$\text{NbTiP}_3\text{O}_{12}$  is a diamagnetic ( $d^0$  system) insulator with a filled valence band and an empty conduction band. The valence band is made up of oxygen  $2s$  and  $2p$  orbitals, whereas the conduction band is made up of Nb ( $5s$ ,  $5p$ ) and Ti ( $4s$ ,  $4p$ ) orbitals. Since the color is white, the band gap  $E_g > 3.0$  eV. Further, since the nearest Nb–Ti distances are fairly large (4.6–4.9 Å (13, 14)), the respective metal  $d$ -orbital overlapping does not occur and only localized  $d$ -levels will be present. The measured two-probe resistivity ( $\rho$ ) at 300 K of  $\text{NbTiP}_3\text{O}_{12}$  is indeed high ( $10^9$ – $10^{10}$  Ω cm) as expected (Table I). On the other hand, the metal-insertion compounds when  $A^{n+} = \text{Mg}$ , Zn, Cd, In, Y, etc. (diamagnetic ions) are  $d^1$  systems ( $\text{Nb}^{4+}$  and/or  $\text{Ti}^{3+}$ ) and the compounds are paramagnetic. Further, electronic ( $n$ -type) “hopping” conduction is expected. Accordingly, the measured  $\rho_{300\text{K}}$  values of the metal-insertion compounds are lowered by three to four orders of magnitude ( $10^6$ – $10^7$  Ω cm) (Table I). Resistivity is lowered further when  $A = \text{Ti}$  or  $\text{Nb}$  (Table I) because electron hopping probability is enhanced between two valence states of the same element (e.g., spinel ferrites  $\text{Fe}_3\text{O}_4$  vs  $\text{NiFe}_2\text{O}_4$ ). Indeed, we can expect metallic conduction when  $x$  is increased to 1.0. In the case where  $A = \text{Mg}$  or  $\text{Zn}$ , we may expect ionic contribution to the conductivity but since they are divalent ions (and the Type II sites are not occupied), ionic mobility will be small. On the other hand, we can expect increased ionic contribution when  $A = \text{Li}$  or  $\text{Na}$  ( $x = 1$  or  $2$ ) (16).

### Conclusions

Only representative metals have been tried by us, but it is clear that any electro-positive element of the periodic table can be inserted into the  $\text{NbTiP}_3\text{O}_{12}$  framework structure to give isostructural phases. In this sense, the host network is as versatile as Chevrel phases,  $A_x\text{Mo}_6\text{Ch}_8$  (3–5, 17) and layered transition-metal dichalcogenides (1–3). Preliminary study also indicated that  $A$  metals can be inserted into  $\text{LiTi}_2\text{P}_3\text{O}_{12}$  and  $\text{Ca}_{0.5}\text{Ti}_2\text{P}_3\text{O}_{12}$ —those compounds with partially or completely filled Type I sites—which means that vacancy at the Type I site is not a necessary condition to obtain the metal-insertion phase. Studies can be extended to  $\square\text{MTiP}_3\text{O}_{12}$ ,  $M = \text{Nb}$ ,  $\text{Ta}$ , and  $\text{Sb}$  and in general, to any phase containing chemically reducible  $M$  (or  $M'$ ) ion.

Ionic and mixed (electronic and ionic) conduction,  $d$ – $d$  and  $d$ – $f$  electron interactions and magnetic properties and thermal expansion behavior of the metal-insertion phases are some of the aspects presently being investigated and will be reported elsewhere.

### Acknowledgments

Thanks are due to CSIR and DST, New Delhi, for the award of research grants.

### References

1. F. JELLINEK, *Arkiv Kemi*, **20**, 447 (1963); *MTP Int. Rev. Sci. (Inorg. Chem. Ser. 1)* **5**, 339 (1972).
2. G. V. SUBBA RAO AND M. W. SHAFER, in “Intercalated Layered Materials” (F. Levy, Ed.), Vol. 6, p. 99, Reidel, Dordrecht (1979).
3. R. SCHÖLLHORN, *Angew. Chem. Int. Ed. Engl.* **19**, 983 (1980); in “Inclusion Compounds” (J. L. Atwood *et al.*, Eds.), Academic Press, New York (1983).
4. G. V. SUBBA RAO AND G. BALAKRISHNAN, *Bull. Mater. Sci. (India)* **6**, 283 (1984); G. V. SUBBA RAO, *Proc. INSA (India)* **A 52**, 292 (1986).
5. J. M. TARASCON, F. J., DiSALVO, D. W. MURPHY, G. W. HULL, E. M. RIETMAN, AND J. V. WASZCZAK, *J. Solid State Chem.* **54**, 204 (1984).

6. D. W. MURPHY, F. J. DISALVO, J. N. CARIDES, AND J. V. WASZCZAK, *Mater. Res. Bull.* **13**, 1395 (1978); I. J. DAVIDSON AND J. E. GREEDAN, *J. Solid State Chem.* **51**, 104 (1984).
7. J. GALY, B. LAVAUD, A. CASALOT, AND P. HAGENMULLER, *J. Solid State Chem.* **2**, 531 (1970); D. W. MURPHY, P. A. CHRISTIAN, F. J. DISALVO, AND J. V. WASZCZAK, *Inorg. Chem.* **18**, 2800 (1979).
8. M. M. THACKERAY, W. I. F. DAVID, P. G. BRUCE, AND J. B. GOODENOUGH, *Mater. Res. Bull.* **18**, 461 (1983).
9. D. W. MURPHY, J. L. DYE, AND S. M. ZAHURAK, *Inorg. Chem.* **22**, 3679 (1983).
10. A. NADIRI, C. DELMAS, R. SALMON, AND P. HAGENMULLER, *Rev. Chim. Miner.* **21**, 537 (1984); C. C. TORARDI AND E. PRINCE, *Mater. Res. Bull.* **21**, 719 (1986); W. M. REIFF, J. H. ZHANG, AND C. C. TORARDI, *J. Solid State Chem.* **62**, 231 (1986).
11. P. HAGENMULLER AND W. VAN GOOL (Eds.), "Solid Electrolytes," Academic Press, New York (1978); P. VASHISTA, J. N. MUNDY, AND G. K. SHENOY (Eds.), "Fast Ion Transport in Solids—Electrodes and Electrolytes," North-Holland, New York (1979).
12. C. N. R. RAO (Ed.), "Advances in Solid State Chemistry, INSA, New Delhi, Proceedings, INSA Golden Jub. Symp.," (1986); C. N. R. RAO AND J. GOPALAKRISHNAN, "New Directions in Solid State Chemistry," Cambridge Univ. Press, Cambridge (1986).
13. L. O. HAGMAN AND P. KIERKEGAARD, *Acta Chem. Scand.* **22**, 1822 (1968); M. SLJUKIC, B. MATKOVIC, AND B. PRODIC, *Zeit. Kristal.* **130**, 148 (1969).
14. R. MASSE, A. DURIF, J. C. GUITEL, AND I. TORDJMAN, *Bull. Soc. Fr. Minéral. Cristallogr.* **95**, 47 (1972).
15. T. OOTA AND I. YAMAI, *J. Amer. Ceram. Soc.* **69**, 1 (1986).
16. U. V. VARADARAJU, K. A. THOMAS, B. SIVASANKAR, AND G. V. SUBBA RAO, *J. Chem. Soc., Chem. Commun.*, in press.
17. A. M. UMARJI, G. V. SUBBA RAO, M. P. JANAWADKAR, AND T. S. RADHAKRISHNAN, *J. Phys. Chem. Solids* **41**, 421 (1980).
18. J. P. BOILOT, J. P. SALANIE, G. DESPLANCHES, AND D. LEPOTIER, *Mater. Res. Bull.* **14**, 1469 (1979).
19. M. BARJ, H. PERTHUIS, AND PH. COLOMBAN, *Solid State Ionics* **11**, 157 (1983); M. K. RADIONOV, M. P. EVTUSHENKO, N. I. PAVLOVA, AND I. S. REZ, *Kr. Khim. Zh.* **50**, 455 (1984) (*Chem. Abstr.* **101**, 140064c (1985)); A. MBANDZA, E. BORDES, AND P. COURTINE, *Mater. Res. Bull.* **20**, 251 (1985).